

UDK: 53.086; 665.7.035.8

## Firing Variables and Strain Sensitivity of $\text{Bi}_2\text{Ru}_2\text{O}_7$ Thick Resistive Films

Ivanka Stanimirović<sup>\*)</sup>, Zdravko Stanimirović

Vinča Institute of Nuclear Sciences, University of Belgrade Mike Petrovića Alasa 12-14, 11351 Belgrade, Republic of Serbia

---

### Abstract:

*In order to provide accurate and semi-real-time information about performances and conditions of various civil engineering structures thick-film resistors are often being used as strain sensors. For that purpose,  $\text{Ba}_2\text{Ru}_2\text{O}_7$  thick resistive films based on compositions with sheet resistivities of 1 kOhm/sq, 10 kOhm/sq and 100 kOhm/sq were evaluated. Resistors were fired at three different peak temperatures (825°C, 850°C and 875°C) and with three different dwelling times (5 min, 10 min and 15 min) in order to correlate influence of firing variables and thick resistive film strain sensitivity by tracking structure-related changes in resistance, gage factor and noise index values. For 10 kOhm/sq composition values of resistance change vs. temperature and temperature coefficient of resistance were measured and calculated.*

**Keywords:** *Thick resistive film; Firing; Microstructure; Gage factor; Electrical properties.*

---

### 1. Introduction

In an era of small size devices, high reliability and integration, novel applications of thick-film technology such as various thick-film sensing devices and ceramic MEMS induced the need of reassessment of standard procedures used in their realization. In recent years, sensor networks for structural health monitoring often used thick resistive films in collecting information about the degree of strain in estimating risks of structural damage and collapse. In order to provide accurate and semi-real-time information about performances and conditions of various civil engineering structures (buildings, bridges, roads, etc.) thick resistive films are being used as strain sensors because of their good strain sensitivity, stability, reliability and low manufacturing costs [1-3]. Since thick-film strain sensors for structural health monitoring are usually deployed on primary locations, such as columns, walls and ceilings of a building, research efforts have been directed to determining factors that can affect the gauge factor as the key parameter when strain sensors are in question. Several papers dealt with cross-sensitivity of temperature and strain in strain sensing thick resistive films. This is important for structural health monitoring applications because of the day-night and seasonal temperature variations [2,4-5]. Others dealt with materials selection for thick-film strain gauges [6-7].

Having in mind that the key process in formation of these complex structures is the firing process, several authors investigated influence of firing procedure on strain sensitivity of thick resistive films [3,8]. In [3] thick-film resistors with various  $\text{RuO}_2$  concentrations were fired through different firing procedures and relationship between sheet resistivity and gage factor was investigated using model where conductive chains that form the resistor were made

---

<sup>\*)</sup> Corresponding author: [ivanka.stanimirovic@vin.bg.ac.rs](mailto:ivanka.stanimirovic@vin.bg.ac.rs)

of  $n$  resistors in series. In [8] authors determined conductive phase and investigated microstructure of the resistor using two types of X-ray analysis and both scanning and transmission electron microscopy. They measured temperature coefficient of resistivity, resistance and gage factor as a function of three different peak firing temperatures (750, 850 and 950°C) and prolonged firing at 950°C for 6 h.

In order to precisely track and evaluate influence of peak firing temperature and dwelling time on strain sensitivity of  $\text{Bi}_2\text{Ru}_2\text{O}_7$  thick resistive films, this paper aims to correlate firing variables and thick film strain sensitivity by tracking structure-related changes in resistance, gage factor and noise index values.

## 2. Materials and Experimental Procedures

### 2.1 Firing of Thick Resistive Films

Successful firing of thick resistive films requires good understanding of all processes involved in their realization. Thick-film resistor compositions are based on two major ingredients: conductive and insulating phase as well as organic component that burns out during sintering. Conductive phase is usually  $\text{RuO}_2$ , bismuth or lead ruthenates. Insulating phase is borosilicate-based glass. Composition also contains additives such as stabilizers and modifiers of temperature coefficients of resistivity. Rheological characteristics of the thick-film composition are closely related to the screen-printing process that includes screen printer setup, screen choice and preparation, squeegee properties. Prior to sintering, thick films are normally dried in order to evaporate solvents present in the printed film. In an infrared belt type furnace deposited films are being exposed to temperatures of about 150°C in 10 min cycle to secure the solvent removal.

After drying the sintering process takes place. Primary firing conditions are usually based on ink manufacturers recommendations: 30- or 60-min cycle with peak temperature of 850°C for 10 min. Four temperature zones in the belt furnace with independent temperature settings provide five phases of resistor formation:

1. Rise to peak temperature phase (~ 400 - 500°C) - burnout of organic constituents that remained in the film after the drying process.
2. Rise to peak temperature phase (500 - 850°C) - glass melting phase.
3. Peak temperature phase (~ 850°C) – formation of the complex conduction network within the glass matrix.
4. Fall from the peak temperature phase 1 (850 - 400°C) - fast glass solidification.
5. Fall from the peak temperature phase 2 (< 400°C) - annealing and stress relief.

Organic removal requirements control the heating rate and the peak firing temperature is governed by the resistor composition in question. As the firing temperature increases the glass viscosity becomes reduced and formation of complex conduction network within the glass matrix is being initiated. As a result of the sintering process a number of conducting chains is being formed and conducting particles in a chain can be in contact or separated by a thin glass barrier. These formations govern the current flow and, therefore, main conducting mechanisms present in the sintered resistive film are metallic conduction and tunnelling through insulating barriers of metal-insulator-metal structures [9].

### 2.2 Evaluation method

Micro and macrostructural changes that occur in strained thick resistive films can be tracked using standard resources - resistance and noise index measurements [10].

Resistance of the thick resistive film depends on the geometry of the resistor, barrier and contact resistance ( $R_B$  and  $R_C$ , respectively). Under assumption that thick resistive film

consists of  $M$  parallel conducting chains and that each chain contains  $K_C$  contacts between neighbouring conducting particles and  $K_B$  neighbouring particles separated by thin glass barriers, the total resistance can be given by the following expression [11]:

$$R = \frac{K_C}{M^2} R_C + \frac{K_B}{M^2} R_B = \frac{K_C}{M^2} \cdot \frac{\rho}{\pi a} + \frac{K_B}{M^2} \cdot \frac{h^2 s}{q^2 A (2mq\Phi_B)^{1/2}} \cdot \exp\left[\left(\frac{32\pi^2 mqs^2 \Phi_B}{h^2}\right)^{1/2}\right], \quad (1)$$

where  $\rho$  is the specific contact resistance,  $a$  is the radius of the contact between two neighbouring conducting particles,  $q$  and  $m$  are the electron charge and its effective mass,  $h$  is the Planck's constant,  $s$  is the thickness of the insulating layer,  $tg\delta$  is the loss tangent of the insulator,  $A$  is the barrier cross section and  $\Phi_B$  the potential barrier height measured with respect to Fermi energy.

Noise index, measured in a 616 Hz - 1616 Hz range around 1 kHz central frequency also carries information about micro and macro structural changes that take place in the film. Noise index for one frequency decade around central frequency can be given as [12]:

$$NI = 10 \log \frac{\overline{(v^2)}_{12}}{V_{DC}^2}, \quad (2)$$

where:

$$\overline{(v^2)}_{12} = \overline{(v_0^2)}_{12} + \overline{(v_1^2)}_{12} = K_0 K_1 V_{DC}^2 \ln \frac{f_2}{f_1} = K V_{DC}^2 \ln \frac{f_2}{f_1}, \quad (3)$$

and therefore:

$$NI = 10 \log K - 0.157,$$

where parameter  $K = K_0 \cdot K_1$  carries information about the influence of all noise sources present in the sintered thick film. There are two types of noise present.  $f^{-1}$  noise sources are sintered contacts between neighbouring conducting particles and metal-insulator-metal structures due to the Nyquist noise modulation, while Lorentzian terms appear due to fluctuations in number of electrons captured by traps in insulating layers of metal-insulator-metal structures. In the absence of any other noise sources other than  $f^{-1}$ , noise index carries information about micro and macro structural properties of the resistive film through parameter  $K_0$ :

$$K_0 = K_{0C} + K_{0B} = \frac{1}{N_C} \cdot \frac{1}{\left(1 + \frac{N_B R_B}{N_C R_C}\right)^2} \cdot \frac{\alpha_H}{V_{eff} n} + \frac{1}{N_B} \cdot \frac{1}{\left(1 + \frac{N_C R_C}{N_B R_B}\right)^2} \cdot \frac{4\pi m q k T}{3\Phi_B h^2} \cdot tg\delta \cdot \frac{s^2}{C} \quad (4)$$

and Lorentzian terms express their influence through:

$$K_1 = 1 + \frac{1}{K_0 V_{DC}^2 \ln \frac{f_2}{f_1}} \cdot \frac{1}{N_B} \cdot \frac{1}{\left(1 + \frac{N_C R_C}{N_B R_B}\right)^2} \cdot \frac{N_T}{N_B} \cdot \int_{f_1}^{f_2} \frac{8\pi m q^3}{h^2 \Phi_B \epsilon_0^2 \epsilon_r^2} \cdot \frac{s^2 x_1^2}{A^2} \cdot \left(1 - \frac{x_1}{s}\right)^2 \cdot \left[\left(1 - \frac{x_1}{s}\right)^2 + \frac{x_1^2}{s^2}\right] \cdot \frac{\frac{\tau_c}{\tau_e}}{\left(1 + \frac{\tau_c}{\tau_e}\right)^2} \cdot \frac{\frac{1}{\tau_c} + \frac{1}{\tau_e}}{1 + \omega^2 \left(\frac{1}{\tau_c} + \frac{1}{\tau_e}\right)^2} df. \quad (5)$$

where  $\alpha_H$  is the Hooke numerical parameter of the order of  $10^{-3}$ ,  $V_{eff}$  and  $n$  are the effective volume of the sintered contact and free carriers concentration in the contact region, respectively,  $k$  is the Boltzmann's constant,  $T$  is the absolute temperature,  $tg\delta$  is the loss

tangent of the insulator,  $C$  is the capacitance of the metal-insulator-metal structure,  $x_l$  is the position of the trap inside the glass barrier,  $\varepsilon_0$  is the vacuum electrical permittivity,  $\varepsilon_r$  is the electrical permittivity of the glass,  $\tau_c$  is the electron capture time parameter and  $\tau_e$  is the electron emission time parameter.

Therefore, changes of the noise index for equally strained resistors formed using different firing variables can be evaluated using:

$$\Delta(NI) \approx \frac{10}{\ln(f_2/f_1)} \left( \frac{\Delta K_0}{K_0} + \frac{\Delta K_1}{K_1} \right), \quad (6)$$

and based on (Eq. 1) accordingly:

$$\Delta R \approx \frac{R_C}{M} \Delta K_C + \frac{K_C}{M} \Delta R_C + \frac{R_B}{M} \Delta K_B + \frac{K_B}{M} \Delta R_B - \frac{R}{M} \Delta M. \quad (7)$$

### 2.3 Experiment

In order to analyse effects of thermal processing on properties of the thick resistive film for strain sensing applications, three groups of thick-film resistors of different sheet resistances and identical geometries (Fig. 1) were subjected to different firing conditions. All tested samples were formed on 96 % pure alumina ( $\text{Al}_2\text{O}_3$ ) [13-14] substrates using conventional screen-printing techniques. Resistive films were 21 mm long and 3 mm wide. Six pads that divided each resistor into 7 identical sequences ( $3 \times 3 \text{ mm}^2$ ) were assigned for additional electrical measurements in future investigations.

Resistors were realized using commercially available resistor compositions based on  $\text{Bi}_2\text{Ru}_2\text{O}_7$  with nominal sheet resistances of 1  $\text{k}\Omega/\text{sq}$ , 10  $\text{k}\Omega/\text{sq}$  and 100  $\text{k}\Omega/\text{sq}$  in combination with Pd/Ag conductor composition. Conventional screen-printing process was performed using 200-mesh stainless steel screens with emulsion thicknesses of 10-12  $\mu\text{m}$ . Conductor print was dried and fired prior to resistor screen printing. In order to obtain desired thicknesses of dry resistive layers of 25  $\mu\text{m}$ , wet resistive layers were 36-38  $\mu\text{m}$  thick depending on composition in question. After the screen-printing process, all of the wet layers were levelled for 15 min at the room temperature and dried in the conveyer infrared drier using 10 min/150°C cycle. To avoid any occurrence of blisters, cracks or crazing, dried resistive layers were closely examined.

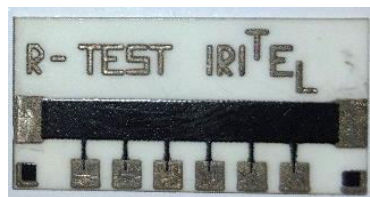


**Fig. 1.** Thick-film resistors used in experimental investigations.

Since the key properties of thick-resistive film are determined by reactions that take place during firing in high temperature zone of the kiln, firing conditions were closely monitored. Air flow rates were checked and every substrate experienced the same air flow regardless of its position on the furnace belt. Temperature control system of the furnace provided accurate temperature settings for each zone and constancy over the realisation periods in order to eliminate possible reliability issues. During the rise to peak temperature firing phase (~ 400-500°C), trapping of the organic constituent due to incomplete burnout of remaining organic constituents can take place. It can lead to bubble formation (500-850°C)

and affect homogeneity of the resistive film. Unstable peak temperature and/or varying dwelling time in the peak zone can affect resistive film structure formation. Too fast glass solidification during the fall from the peak temperature ( $\sim 800\text{--}400^\circ\text{C}$ ) may induce stress in the film that may contribute to abnormal values of resistor noise. Stress induced by the fast glass solidification may be partially annealed out during the annealing and stress relief phase ( $< 400^\circ\text{C}$ ). All those issues can detriment resistivity, noise and strain sensing performances of the fired resistive film.

Having in mind that that temperature distribution of the unloaded furnace differs from that of the loaded one, experimental results were recorded under following conditions:

- sufficient time was allowed for furnace to reach and stabilize pre-set temperatures in all 9 zones (Fig. 2a and 2b)
- the belt was uniformly loaded,
- before each firing cycle sufficient number of blank substrates had passed through the hot zone and equilibrium was achieved,
- temperature profiles were checked using control thermocouples attached to the dummy loads (Fig. 2c).

Also, the transit rate of samples through the furnace were uniform and provided adequate resistor firing profiles.

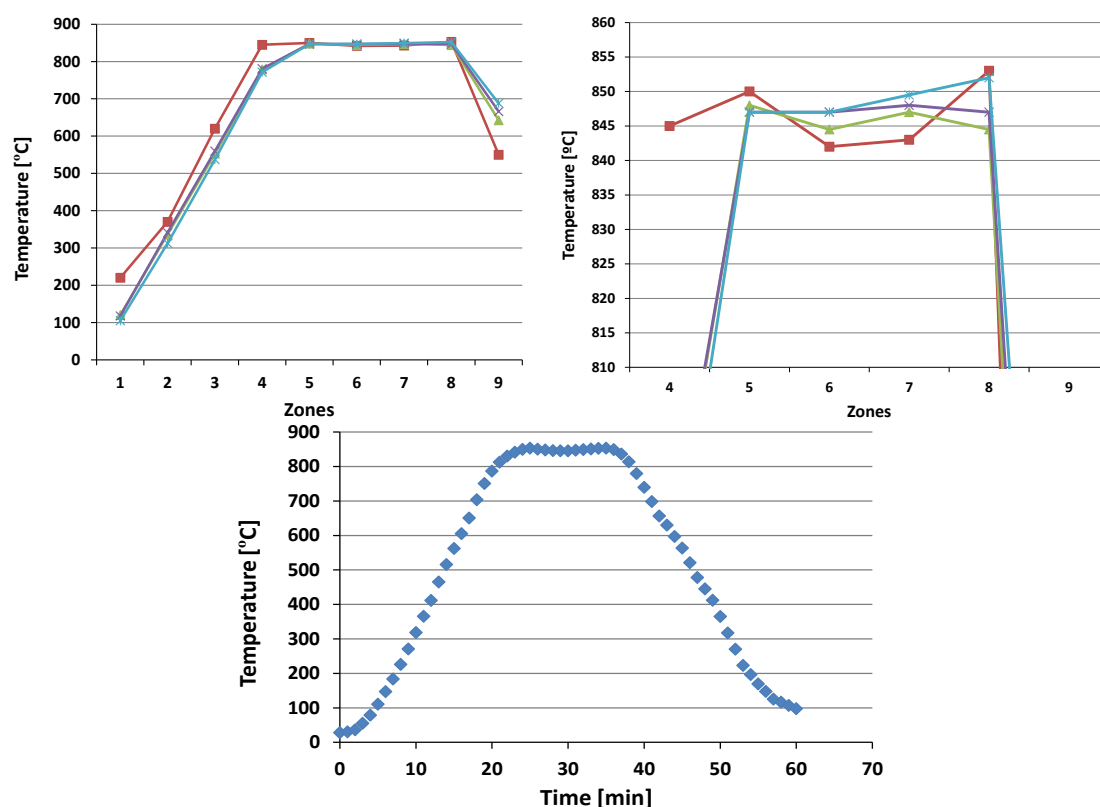


**Fig. 2.** Setting of the primary 60 min cycle firing profile (a) and the peak temperature of  $850^\circ\text{C}$  for 10 min (b) and stabilized primary firing profile obtained using control thermocouple attached to the dummy load (c).

For experimental purposes three firing profiles were chosen: primary profile recommended by the composition manufacturer with peak temperature of  $850^\circ\text{C}$ , as well as two profiles with lower ( $825^\circ\text{C}$ ) and higher peak ( $875^\circ\text{C}$ ) temperature. For recommended temperature profile, effects of time spent at the peak temperature were examined for three

different dwelling times: 5 min, 10 min (recommended by the resistive composition manufacturer for the optimum structure formation) and 15 min. Simulation of straining was performed using custom made device that allowed substrate deflection of up to 300  $\mu\text{m}$  – maximum reliably obtainable deflection for substrate material in question. Resistive film was centrally positioned on a substrate that was fixed on both ends providing maximum straining.

Gage factor  $GF$  of the resistive film, as a measure of the strain sensitivity, was calculated using [12]:

$$GF = \frac{\Delta R}{R\varepsilon_{\max}} = \frac{\Delta Rl}{R\Delta l} = \frac{\Delta RL^2}{6Rdt}, \quad (8)$$

where  $\Delta l/l$  designates the relative change of the film length due to substrate deflection  $d$ ,  $t$  is the substrate thickness and  $L$  is the distance between fixed substrate ends.

Structural health monitoring applications require measurements of cross-sensitivity of temperature and strain. This is important for structural health monitoring applications because of seasonal and day-night temperature variations. Temperature coefficient of the resistance ( $TCR$ ) was calculated using:

$$TCR = \frac{R(T_2) - R(T_1)}{R(T_1) \times (T_2 - T_1)} \times 10^6, \quad (9)$$

where  $R(T_i)$  represents film resistance  $R$  at specific temperature  $T_i$ .

All test samples were realized and all measurements were performed at Institute for telecommunications and electronics IRITEL a.d. Belgrade, Serbia. HP34401A instrument was used for resistance measurements and Quan-Tech Resistor Test Set, Model 315B was used for noise index measurements at 1 kHz.

### 3. Results and Discussion

In order to analyse influence of the peak firing temperature on straining performances of fired thick resistive films, three peak firing temperatures were chosen: recommended peak temperature of 850°C and peak temperatures lower (825°C) and higher (875°C) than the optimum one with 10 min optimum dwelling times at peak temperature for the chosen firing temperature profile.

When recommended peak temperature of 850°C is in question, main requirements for successful structure formation were met and measured resistance and noise index values were used as reference values. Previous investigations [12] showed that mechanical straining causes reversible resistance change partially due to geometrical, but mainly due to microstructural changes. Gage factors of about 2-2.5 are due to geometrical factors [8]. Greater gage factors depend on changes in the microstructure of the resistive film. During firing complex random conductive network is being formed. Spatially uneven insulating and conductive phase distribution leads to random formation of conducting chains and glass areas. Compositions with high conductive/glass phase ratio have metallic conduction as the dominant conduction mechanism. Tunnelling through glass barriers is the dominant conduction mechanism for compositions with low conductive/glass ratio, such as 100 kOhm/sq. Resistors with 1 kOhm/sq sheet resistivity have high content of conductive phase and conduction through clusters of conducting particles and sintered contacts governs the current flow. 10 kOhm/sq composition incorporates both types of conduction mechanisms. Straining changes charge transport conditions in resistor. Conducting phase in thick-film compositions is far stiffer than the insulating one [15]. Mechanical straining cannot change number of contacts  $K_C$ , barriers  $K_B$  and conducting chains  $M$  formed during firing. It doesn't affect contact resistance  $R_C$  but changes barrier resistance  $R_B$  by affecting the barrier width  $s$  (Eq. 7). When noise index is in question straining affects both  $f^{-1}$  noise sources and

Lorentzian terms through changes in parameters  $K_0$  and  $K_1$  that are caused by alterations in  $s$  and consequentially in  $R_B$  (Eq. 8). Peak temperature lower than the recommended one ( $825^\circ\text{C}$ ) lowered resistance values for resistors formed using 10 kOhm/sq and 100 kOhm/sq resistors. 1 kOhm/sq composition has a high-volume fraction of conducting phase and therefore lower peak firing temperature couldn't significantly affect formation of conducting chains in the resistive film. Thick resistive film based on 10 kOhm/sq composition obtained resistance values slightly lower than optimum ones. Although 10 kOhm/sq resistors have balanced volume fractions of conducting and insulating phase, certain number of conducting particles wasn't completely immersed in insulating glass matrix and therefore number of conducting chains was greater than optimum. 100 kOhm/sq resistors had resistance values significantly lower than designed because of the low volume fraction of conducting phase and high volume fraction of insulating phase. At the peak temperature of  $825^\circ\text{C}$  conducting phase was not fully immersed in the insulating glass matrix. Therefore, the greater number of adjacent conducting particles remained in contact or separated by a thin glass barrier that allowed tunnelling conduction. As a result, a greater number of conducting chains was formed. Random resistor networks formed at this temperature exhibited lower resistance values than resistors fired at the recommended peak temperature.

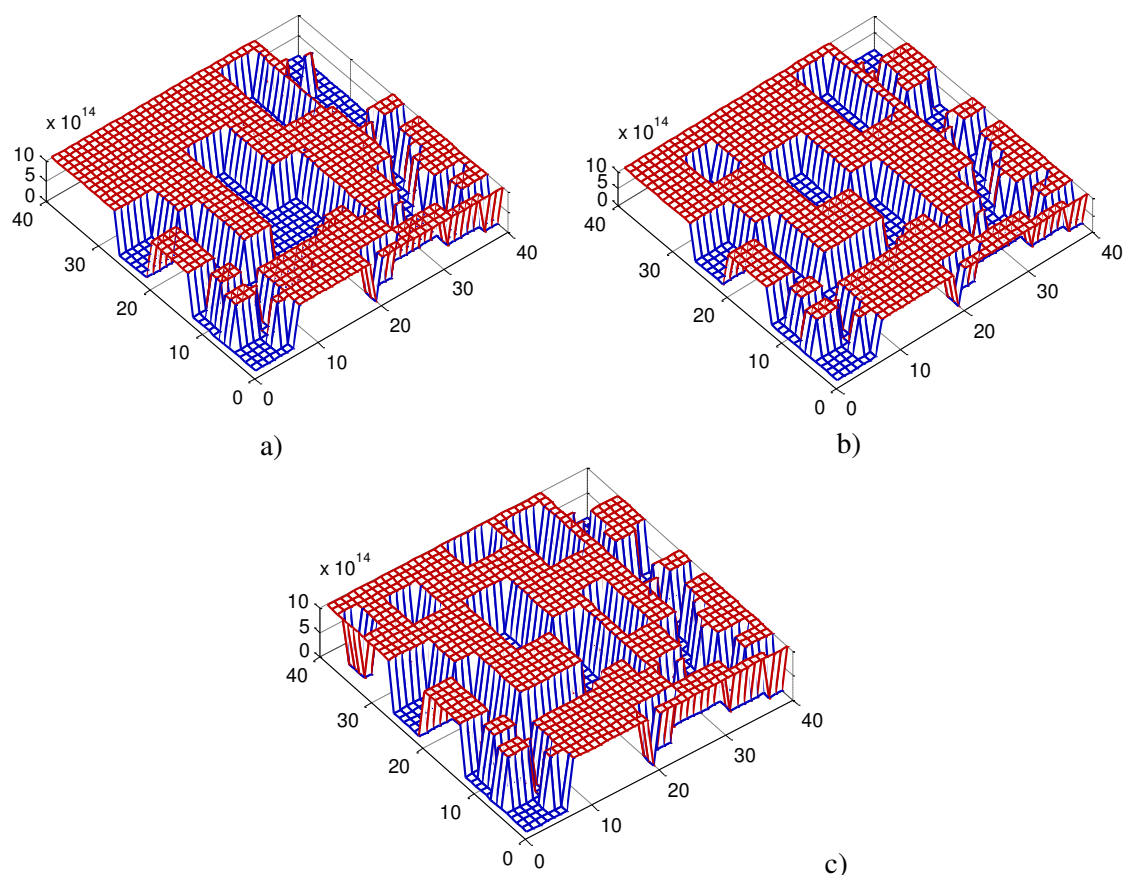


**Fig. 3.** Evolution of the 10 kOhm/sq thick resistive film structure with the increase in peak temperature:  $825^\circ\text{C}$  - conducting phase was not fully immersed in the insulating glass matrix,  $850^\circ\text{C}$  - structure formed under recommended conditions,  $875^\circ\text{C}$  - reduced glass viscosity led to greater immersion of conducting particles into glass matrix.

Peak temperature higher than the recommended one ( $875^\circ\text{C}$ ) had little effect when 1 kOhm/sq composition is question because of its high metallic content. 10 kOhm/sq

composition behaved differently. Reduced glass viscosity led greater immersion of conducting particles into glass matrix and therefore reduced the number of conducting chains in the resistive film. Consequently, it affected metallic and tunneling conduction processes. 100 kOhm/sq composition was affected the most. Low volume fraction of conducting phase and high insulating glass content in combination with higher peak temperature caused greater immersion of conducting phase in the glass matrix that led to significantly reduced number of conducting chains because of increased number of glass barriers that formed between adjacent conducting particles. Random resistor networks formed at this temperature exhibited higher resistance values than resistors fired at the recommended peak temperature of 850°C.

Evolution of the 10kOhm/sq thick resistive film structure with the increase in peak temperature is illustrated with Fig. 3. 10 kOhm/sq composition was selected because it equally incorporates both types of conduction mechanisms: metallic conduction and tunnelling through glass barriers.

Gage factor measurements showed that  $GF$  exhibit higher values for compositions with higher sheet resistivities and that  $GF$  decreases with the increase in temperature for the same composition. Measured resistance and  $GF$  values of strained thick resistive films fired at three different peak temperatures for 10 min are shown in Fig. 4.

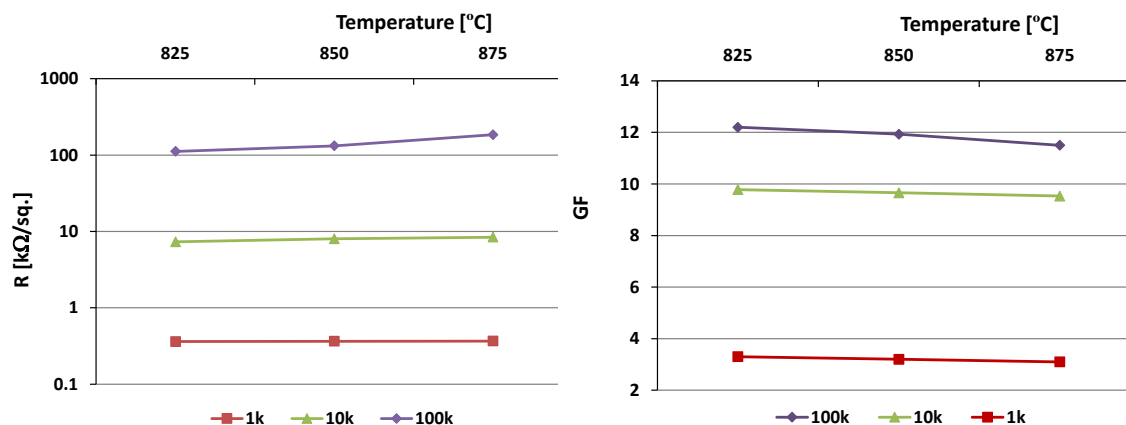


**Fig. 4.** Resistivities (a) and gage factor (b) values of strained thick resistive films fired at three different peak temperatures for 10 min.

In order to analyse influence of the dwelling time on the peak firing temperature on strain sensitivity of fired thick resistive films, three dwelling times were chosen: 5 min, 10 min (recommended) and 15 min.

For all examined compositions dwelling time of 5 min at recommended peak temperature of 850°C was insufficient to affect resistor structure formed at the recommended peak temperature. Time was insufficient to induce further spatial distribution of conducting particles and increase in number of conducting chains.

Optimum dwelling time of 10 min at optimum firing temperature gave expected resistor properties for all three compositions. Number of conducting chains was in accordance with sheet resistivities of used resistor compositions [9].

Longer dwelling times (15 min) significantly affected only 100 kOhm/sq composition. Further spatial distribution of the conducting phase within the glass matrix took place and resulted in reduction of conducting chains due to thicker glass barriers between adjacent conducting particles. That led to resistance increase and  $GF$  decrease. Measured resistance and  $GF$  values of strained thick resistive films fired at peak temperature of 850 °C for 5 min, 10 min and 15 min are shown in Fig. 5.



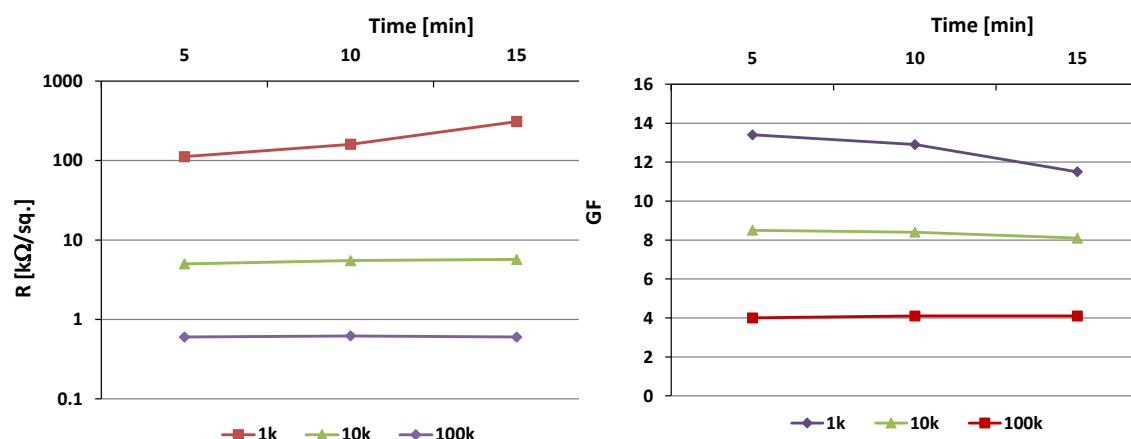


**Fig. 5.** Resistivities (a) and gage factor (b) values of strained thick resistive films fired at peak temperature of 850°C for 5 min, 10 min and 15 min.

Noise index values slightly increased with the increase in peak temperature and dwelling time for the same composition. For 1 kOhm/sq composition measured  $NI$  values were about -24.2 dB, for 10 kOhm/sq composition about -15.1 dB and for 100 kOhm/sq composition about -6.3 dB.

Obtained results showed that resistive films realized using 10 kOhm/sq composition have stable  $GF$  values and relatively low noise and therefore are suitable for strain sensing applications. Structural health monitoring requires employing strain sensors with low-temperature sensitivity, so  $TCR$  values for strained thick resistive film fired at three different peak temperatures for temperatures of 25°C and 125°C were calculated (Fig. 6).

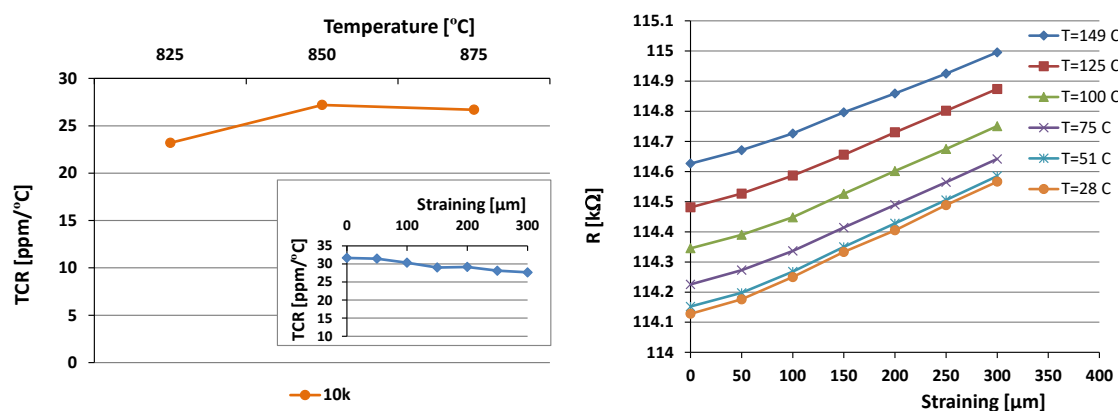


**Fig. 6.**  $TCR$  values of strained 10 kOhm/sq thick resistive film fired at peak temperature of 850°C for 5 min, 10 min and 15 min. Inset: resistance change vs. temperature for thick resistive film fired at 850°C and subjected to straining in the range of 0  $\mu\text{m}$  to 300  $\mu\text{m}$  (a) and resistance change vs. temperature for 10 kOhm/sq thick resistive film fired at peak temperature of 850°C for 10 min and subjected to straining in the range of 0  $\mu\text{m}$  to 300  $\mu\text{m}$  (b).

Results presented in Fig. 6a show that  $TCR$  does not significantly depend on firing conditions and the applied load and that  $TCR$  value of the thick-film are close to constant. It should be pointed out that strain sensors for structural health monitoring operate at ambient temperatures and, as an example, road temperatures in dry hot areas do not exceed 70°C [16].

Higher temperatures cannot affect operation of the strained thick resistive films (Fig. 6b) since softening of the glass phase requires temperatures close to 500°C.

#### 4. Conclusion

Thick-film resistors based on  $\text{Ba}_2\text{Ru}_2\text{O}_7$  for application in structural health monitoring were evaluated in order to correlate firing variables and strain sensitivity of thick resistive films. Simulation of straining was performed using custom made device that provided  $\text{Al}_2\text{O}_3$  deflection of 300  $\mu\text{m}$  – maximum reliably obtainable deflection for the substrate material in question. Resistors of three different sheet resistivities, 1kOhm/sq, 10 kOhm/sq and 100 kOhm/sq, were fired at three different peak temperatures (825, 850 and 870°C) for 10 min and with three different dwelling times (5, 10 and 15 min) at 850°C to determine the influence of firing variables on structure-related changes in resistance, gage factor and noise index values. Peak firing temperature of 850°C with 10 min dwelling time is the recommended temperature profile and therefore the main requirements for successful structure formation were met. Measured resistance and noise index values were used as reference values. At the peak temperature of 825°C conducting phase was not fully immersed in the insulating glass matrix. At the peak temperature of 875°C reduced glass viscosity led to the greater immersion of conducting particles into the insulating glass. Alteration in peak temperatures had little effect when 1 kOhm/sq composition was question because of its high metallic content. 10 kOhm/sq and 100 kOhm/sq resistors had resistance values lower than reference ones after firing at a peak temperature of 825°C. Peak firing temperature higher than recommended resulted in increase of their resistance. Gage factors for all three compositions decreased with the increase in peak firing temperature.

Change of dwelling times affected 100 kOhm/sq resistors the most and they exhibited the greatest increase of the resistance value with the increase of dwelling time at 850°C because of the prolonged spatial distribution of the conducting phase within the glass matrix.  $GF$  decreased with the increase of dwelling time.

Noise index values slightly increased with the increase in peak temperature and dwelling time for the same composition and were around -24.2 dB for 1 kOhm/sq, around -15.1 dB for 10 kOhm/sq composition and around -6.3 dB for 100 kOhm/sq composition.

The main structure-related parameter responsible for observed behaviour was the barrier width  $s$  that affects tunnelling through glass barriers that form between adjacent conducting particles during firing process. Therefore, change in the barrier resistance  $R_B$  causes resistance, gage factor and noise index values alterations.

Obtained results showed that thick resistive films realized using 10 kOhm/sq compositions have stable  $GF$  values and relatively low noise and therefore are suitable for structural health monitoring strain sensing applications. Their  $TCR$  does not significantly depend on firing conditions and the applied load and  $TCR$  values of the strained thick-film are close to constant. When structural health monitoring at high ambient operating temperatures is in question their performances excel because softening of the glass phase requires temperatures close to 500°C.

#### Acknowledgments

Authors would like to thank the Institute for telecommunications and electronics IRITEL a.d. Belgrade, Serbia, where all test samples were realized and all measurements were performed.

## 5. References

1. S.A.A. Jabir, N.K. Gupta, Thick-Film Ceramic Strain Sensors for Structural Health Monitoring, *IEEE transactions on instrumentation and measurement*, 60(11) (2011) 3669-3676.
2. M. Wen, X. Guan, H. Li, J. Ou, Temperature characteristics of thick-film resistors and its application as a strain sensor with low temperature-sensitivity, *Sensors and Actuators A: Physical*, 31 (2020).
3. X. Guan, M. Wen, H. Li, J. Ou, The influence of firing procedures on strain sensitivity of thick-film resistors, *Ceramics International*, 45 (2019) 6836-6841.
4. Y. Zheng, J. Atkinson, R. Sion, Z. Zhang, A study of some production parameter effects on the resistance-temperature characteristics of thick film strain gauges, *J. Phys. D: Appl. Phys.*, 35 (2002) 1282-1289.
5. Y. Zheng, J. Atkinson and R. Sion, An explanation of thermal behaviour of thick film strain gauges, *J. Phys. D: Appl. Phys.*, 36 (2003) 1153-1158.
6. M. Hrovat, D. Belavič, Z. Samardžija, J. Holc, A characterisation of thick film resistors for strain gauge applications, *Journal of Materials Science*, 36(11) (2001) 2679-2689.
7. M. Hrovat, D. Belavič, A. Benčan, J. Bernard, J. Holc, J. Cilenšek, W. Smetana, H. Homolka, R. Reicher, L. Golonka, A. Dziedzic, J. Kita, Thick-film resistors on various substrates as sensing elements for strain-gauge applications, *Sensors and Actuators A: Physical*, 107(3) (2003) 261-272.
8. M. Hrovat, A. Bencan, D. Belavič, J. Holc, G. Dražić, The influence of firing temperature on the electrical and microstructural characteristics of thick-film resistors for strain gauge applications, *Sensors and Actuators A Physical*, 103(3) (2003) 341-352.
9. M.M. Jevtić, Z. Stanimirović, I. Stanimirović, Evaluation of thick-film structural parameters based on noise index measurements, *Microelectronics Reliability*, 41 (2001) 59-66.
10. Stanimirović, Z. Stanimirović, Influence of HVP trimming on primary parameters of thick resistive films, *J Mater Sci: Mater Electron*, 28 (2017) 8002-8010.
11. M.M. Jevtić, Z. Stanimirović, I. Mrak, Low-Frequency Noise in Thick-Film Resistors due to Two-Step Tunneling Process in Insulator Layer of Elemental MIM Cell, *IEEE Transactions on Components, Packaging, and Manufacturing Technology-Part A*, 22(1) (1999) 120-125.
12. Z. Stanimirović, M.M. Jevtić, I. Stanimirović, Simultaneous Mechanical and Electrical Straining of Conventional Thick-Film Resistors, *Microelectronics Reliability*, 48 (2008) 59-67.
13. Durmuş, Gul, Çömez, Uzun, From metal chips to composite: Effect of age-hardening on mechanical and wear properties of Al<sub>2</sub>O<sub>3</sub> reinforced AA7075 composites, *Science of Sintering*, 52(2) (2020) 177-186.
14. Davodi, Ardestani, Kazemi, Sinterability and characterization of Ag/Al<sub>2</sub>O<sub>3</sub> metal and ceramic matrix composites processed by mechanical milling, *Science of Sintering*, 52(3) (2020) 245-255.
15. C. Grimaldi, P. Ryser, S. Strassler, Gauge Factor Enhancement Driven by Heterogeneity in Thick-Film Resistors, *J. Appl. Phys.*, 91(1) (2001) 322-327.
16. N. Solatifar, M. Abbasghorbani, A. Kavussi, H. Sivilevičius, Prediction of depth temperature of asphalt layers in hot climate areas, *Journal of Civil Engineering and Management*, 24 (2018) 516-525.

---

**Сажетак:** Да би се добила тачна информација у приближно реалном времену о перформансама и стању различитих грађевинских објеката, као сензори напрезања се често користе дебелослојни отпорници. Из тог разлога извршено је истраживање везано за дебеле отпорне филмове на бази  $Va_2Ru_2O_7$  слојних отпорности 1 kOhm/sq, 10 kOhm/sq и 100 kOhm/sq. Жарење отпорника се одвијало при различитим максималним температурама жарења (825, 850 и 875°C) и при различитим временима проведеним на максималној температури жарења (5, 10 и 15 минута) да би се повезао утицај варијабли жарења на осетљивост дебелослојних отпорника на напрезање праћењем структурних промена које се огледају у вредностима отпорности, фактора напрезања и индекса шума. За 10 kOhm/sq отпорнике мерене су и рачунате вредности промене отпорности са напрезањем и температурног коефицијента отпорности.

**Кључне речи:** Дебели отпорни филм, жарење, микроструктура, фактор напрезања, електрична својства.

---

© 2022 Authors. Published by association for ETRAN Society. This article is an open access article distributed under the terms and conditions of the Creative Commons — Attribution 4.0 International license (<https://creativecommons.org/licenses/by/4.0/>).

